Journal for Technology of Plasticity, Vol. 34 (2009), Number 1-2

DETERMINATION OF WORKING STRESS AND LIMITING FLANGING RATIO IN THE HOLE-FLANGING PROCESS OF SHEET METAL BLANKS

Velibor Marinković
University of Niš, Faculty of Mechanical Engineering, Serbia

ABSTRACT

The paper presents an analysis of the conventional hole-flanging process based, on one hand, on a purely theoretical base and, on the other hand, on the experimental one. The original formulae for calculating working stress (force) of the hole-flanging are derived. The theoretical results are compared to the experimental ones thereby their satisfying compliance is identified. Further on, other important parameter of the hole-flanging process-limiting flanging ratio-is also theoretically and experimentally analyzed. For experimental research, a representative high-alloyed stainless steel known for its high cold formability is chosen. The experiment was carried out under the most difficult frictional conditions, that is, with no use of lubricant. The recommendations to meet the needs of engineering calculations are given.
Key Words*: Hole-flanging Process, Working Stress (Force), Limiting Flanging Ratio*

1. INTRODUCTION

Sheet metal forming processes, including blanking, drawing, bending and flanging are extensively applied in industry. Flanging can be divided into several sub-operations: hole-flanging, stretch flanging, shrink flanging, straight flanging (bending), reverse flanging and jogged flanging.
Hole-flanging is one of the most important forming processes widely used for producing sheet metal components in the automotive and electrical-product industries. This process of sheet metal forming is mainly used for two purposes, namely, (a) for increasing rigidity of various sheet metal parts (structures), and (b) for neck formation on sheet metal parts and tubes in order to connect them with other elements (directly or by means of subsequently cut thread).

This study is focused on the conventional hole-flanging process. As it is well-known, the conventional hole-flanging process in which a free part of the sheet metal blank with a small hole in its center, under the impact of the punch, is drawn into the die orifice in order to shape the hole-flanged part (Fig. 1).

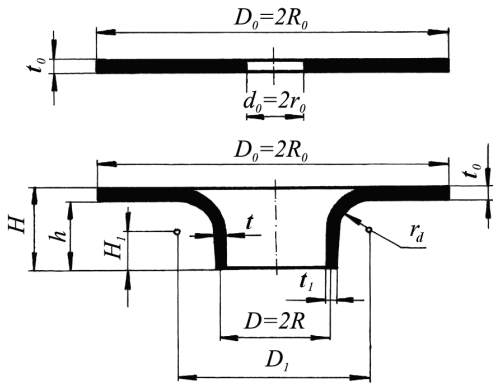

Fig.1 - Geometrical Parameters of the Blank and the Finished Part

During the hole-flanging process, the diameter of the initial hole constantly increases, just like the height of the flanged (extruded) neck while the wall thickness constantly decreases. The previously determined small hole in the center of the flat circular sheet metal is often formed by piercing. The operations of piercing and hole-flanging can be realized successively. In that case a conical punch is used unlike a flat-headed one which is used for the conventional process of hole - flanging. This technological procedure provides for higher economy and height of the flanged neck (due to the absence of scrap) but, at the same time, its smaller geometrical accuracy and surface quality. Rough places along the edge of the flanged neck require subsequent cutting treatment. Finally, piercing can also induce initial cracks along the edge of the flanged neck which may give rise to plastic fracture of the finished part in the hole-flanging phase.
Hole-flanging and related processes have been investigated analytically and experimentally [1], [2], [3], [4], [5], [6], [7], [8], [9], [10]. Conventional hole-flanging process is constrained by the formability of sheet metals and quality of the cut surface in piercing process, which normally used as the first step in the hole-flanging operations. Some studies have been conducted on the above-mentioned problems [11], [12], [13].

2. THEORETICAL APPROACH

2.1.Hole-flanging Working Stress

In order to determine the working stress of hole-flanging process it is necessery to define the stress and strain state in the zone of plastic deformation (ZPD). Stress-strain state is variable during the process as well as in ZPD. Regarding stress-strain state, hole-flanging belongs to complex forming processes. Also, hole-flanging represents a typical example of non-stationary forming process. Starting from the expressions for defining the components of the strain tensor as well as from the equations of equilibrium in the generalized coordinates, Marinkovic [14] has formulated corresponding formulae for curvilinear (toroidal) coordinates.

The process of the hole-flanging belongs to the problems of axisymmetrical forming (Fig. 2), for which the next equations are valid ($\tau_{\rho\theta} = \tau_{\theta} = \gamma_{\rho\theta} = \gamma_{\theta} = 0$) [14]:

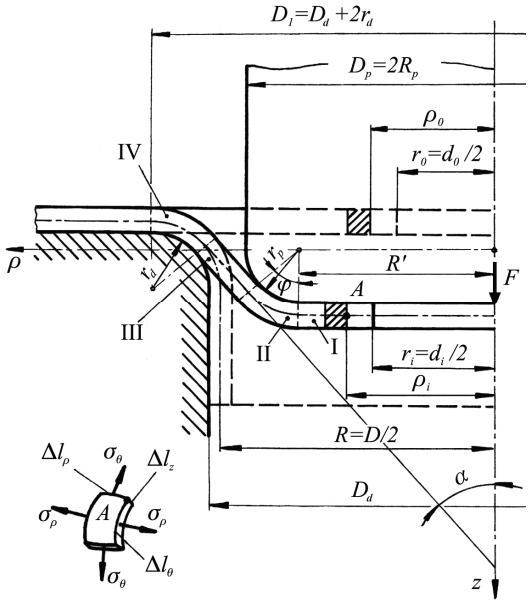

Figure 2 - Scheme of the Hole-flanging Process

$$\varepsilon_\rho = \frac{\partial u_\rho}{\partial \rho} \tag{1a}$$

$$\varepsilon_\theta = \frac{1}{R' \pm \rho \sin} + \frac{\partial u_\theta}{\partial \theta} \pm \frac{\sin\varphi\, u_\rho + \cos\varphi\, u_\varphi}{R' \pm \rho \sin} \tag{1b}$$

$$\varepsilon_\varphi = \frac{1}{\rho}\frac{\partial u_\varphi}{\partial \varphi} + \frac{u_\rho}{\rho} \tag{1c}$$

$$\gamma_{\rho\varphi} = \frac{\partial u_\varphi}{\partial \rho} - \frac{u_\varphi}{\rho} + \frac{1}{\rho}\frac{\partial u_\rho}{\partial \varphi} \tag{1d}$$

$$\frac{\partial \sigma_\rho}{\partial \rho} + \frac{1}{\rho}\frac{\partial \tau_{\rho\varphi}}{\partial \varphi} \pm \frac{(\sigma_\rho - \sigma_\theta)\sin\varphi}{R' \pm \rho \sin\varphi} + \frac{\sigma_r - \sigma_\varphi}{\rho} \pm \frac{\tau_{\rho\varphi}\cos\varphi}{R' \pm \rho \sin\varphi} = 0 \tag{2a}$$

$$\frac{\partial \tau_{\rho\varphi}}{\partial \rho} + \frac{1}{\rho}\frac{\partial \sigma_\varphi}{\partial \varphi} + \frac{(\pm\sigma_\theta \mp \sigma_\varphi)\cos\varphi}{R' \pm \rho \sin\varphi} + \frac{2\tau_{\rho\varphi}}{\rho} \pm \frac{\tau_{\rho\varphi}\sin\varphi}{R' \pm \rho \sin\varphi} = 0 \tag{2b}$$

While using formulae (1) and (2) care must be taken about geometric relations and algebraic signs right before the stress tensor components.
If in the first approximation the impact of contact friction is neglected, expression (2b) is reduced to a simple equation:

$$\frac{1}{\rho}\frac{\partial \sigma_\varphi}{\partial \varphi} + \frac{(\sigma_\varphi - \sigma_\theta)\cos\varphi}{R' + \rho \sin\varphi} = 0 \tag{3}$$

Since it is an axisymmetrical forming process, the isotropic yield criterion can be expressed in the form:

$$\sigma_\varphi - \sigma_\theta = \overline{\sigma} \tag{4}$$

Assuming that the normal stress at the section I ($\sigma_{\varphi I}$) is known, due to the equations (3) and (4) the folowing relation is obtained (Fig. 2):

$$\int_{\sigma_{\varphi I}}^{\sigma_\varphi} d\sigma_\varphi = \int_0^\varphi \overline{\sigma}\,\frac{\rho \cos\varphi}{R' + \rho \sin\varphi}\, d\varphi\,, \tag{5}$$

After integration the equation (5) is obtained:

$$\sigma_\varphi = \sigma_{\varphi I} + \overline{\sigma}_{ave}\,\ell n\,\frac{R' + \rho \sin\varphi}{R'} \tag{6}$$

On the outer edge of segment I the normal meridian stress achieves its maximal value which is determined by the formula [15]:

$$\sigma_{\varphi I} = \overline{\sigma}_{ave}\left(1 - \frac{r_i}{\rho_i}\right) \tag{7}$$

By introducing relations (7) in equation (6) the following formula for calculating working stress (at the arbitrary moment of the hole-flanging process) is obtained:

$$\sigma_f \equiv \sigma_{\varphi II} = \overline{\sigma}_{ave}\left[1 - \frac{r_i}{\rho_i} + \ell n\,\frac{R' + \rho \cos\alpha}{R'}\right] \tag{8}$$

At the moment of so-called full envelopment of the punch corner ($\alpha = 0^0$) the maximal working stress in the ZPD is achieved (Fig. 2):

$$\sigma_{f\,max} = \overline{\sigma}_{ave}\left[1 - \frac{r_{im}}{R_p - r_p} + \ell n\,\frac{R_p + 0.5\,t}{R_p - r_p}\right] \tag{9}$$

Similarly to the conventional deep drawing process, total working stress of the hole-flanging process is the sum of the forming stress (σ_f) , stress addition due to bending and unbending of the sheet metal blank (σ_b) and friction at the punch corner (σ_μ) [15], [16].

Finally, taking into account additional impact of sheet metal thinning as well as strain hardening, and following the methodology suggested by Popov [17], the following formulae are proposed for the calculation of the maximal working stress of hole-flanging process (Fig. 2):

a) for $r_{im} \le R'$

$$\sigma_{max} = \bar{\sigma}_{ave}\left[1 - \frac{r_{im}}{R_p - r_p} + \ell n \frac{R_p + 0{,}5\bar{t}}{R_p - r_p}\right](1 + 1{,}6\mu) + \bar{\sigma}_0\left[\frac{\bar{t}}{2r_p + \bar{t}}(1 + 1{,}6\mu) + \frac{\bar{t}}{4r_d + 2\bar{t}}\right] \tag{10a}$$

b) for $r_{im} > R'$

$$\sigma_{max} = \bar{\sigma}_{ave}\left[\frac{R_p - r_p}{r_{im}} - 1 + \ell n \frac{R_p + 0{,}5\bar{t}}{R_p - r_p}\right](1 + 1{,}6\mu) + \bar{\sigma}_0\left[\frac{\bar{t}}{2r_p + \bar{t}}(1 + 1{,}6\mu) + \frac{\bar{t}}{4r_d + 2\bar{t}}\right] \tag{10b}$$

Maximal force of hole-flanging process is calculated by a simple formula:

$$F_{max} = \pi d \bar{t} \sigma_{max} \tag{11}$$

To determine the characteristic radius r_{im} approximate relation can be used [15]:

$$r_{im} \cong r_0 + 0.57(r_p + r_d) + 1.57t_0 \tag{12}$$

Regarding small deformation degres, the average value of flow stress at the moment of emergence of maximal working stress can be determined from the folowing relation [8]:

$$\bar{\sigma}_{ave} = 0.5(\bar{\sigma}_0 + \bar{\sigma}) = \bar{\sigma}_0 + 0.5^{n+1} C \left(\ell n \frac{r_{im}}{r_0}\right)^n \tag{13}$$

2.2. Flanging Ratio

The most important parameter of the hole-flanging process, both for the theoretical analysis and the engineering calculations, is the flanging ratio ($\lambda = D / d_0$).

For the rational technological process design it is very important to know the limiting (maximal) value of this parameter. By means of the simplified analysis of the strain state of the hole-flanging process the following relation is obtained [17]:

$$\lambda_{lim} = 1/(1 - \psi_m) \tag{14}$$

Unfortunately, formula (14) has not been sufficiently verified in the experimental way. It is interesting that in most of the experiments done there was a considerably larger flanging ratio realized than that calculated according to formula (14).

An interesting attempt at theoretical generalization has been made by Averkiev [18]. This author has shown that the limiting forming ratio at sheet metal forming processes can be brought into a functional correlation with "*P*-criterion". This criterion represents a specific work of uniform plastic deformation. For the flow curve of form $\overline{\sigma} = \overline{\sigma}_0 + C\,\overline{\varphi}^{\,n}$ "*P*-criterion" is determined according to the following formula:

$$P = \sqrt{\frac{3(1+\bar{r})}{2(2+\bar{r})}}\left[\overline{\sigma}_0 + \frac{(R_m e^n - \overline{\sigma}_0)^2}{R_m e^n (n+1) - \overline{\sigma}_0}\right] n \tag{15a}$$

On the basis of a series of experiments, the above-mentioned author has set up the following semi-empirical relations for various materials and sheet metal thickness:

$$1/\lambda_{lim} = \begin{cases} 0{,}3796 + 20{,}2304/P; & t_r = 3\% \\ 0{,}3477 + 19{,}9620/P; & t_r = 4\% \\ 0{,}3090 + 20{,}8150/P; & t_r = 5\% \\ 0{,}2948 + 19{,}5235/P; & t_r = 10 \div 30\% \end{cases} \tag{15b}$$

The calculation of the LFR according to formulae (15) gives the results that are in better agreement with the experiment, since the relations themselves are based upon experimental data, though in some cases aberrations can be considerable.

3. EXPERIMENTAL RESEACH

3.1. Material, Equipment and Procedure

The experimental research in this paper refers to high-alloy stainless steel Č.4574 (X10CrNiMoTi18-10), that possesses high cold formability. This steel can be considered as representative of the whole group of chromium-nickel-molobdemium austenitic steels. Otherwise, these steels find a wide application in the manufacture of parts, equipment and devices in many branches of industry (nutrition, chemical, pharmaceutical, textile, etc.).
The chemical composition and mechanical/plastic properties of this material are given in Table 1 and Table 2 [8].
To meet the needs of the experimental research the experimental tool with a set of replaceable cylindrical flat-headed punches and dies was designed (Fig. 3).
The research program was carried out on the single-action hydraulic press of the nominal force of 1000 kN. For the ensurance of pure hole-flanging the tool had a suitable blank holder embedded into it. Namely, the sheet metal blanks of ring-like form are rigidly clamped around its periphery by this blank holder in order to prevent slipping in the contact region between the blank and die. The punch-die clearence is equal to the initial sheet metal thickness.
On the other hand, in order to obtain extreme forming conditions no lubricant was used ($\mu \approx 0.22$). The holes on the blanks were obtained by piercing as well as by additional subsequent cutting treatment. Regarding the measuring equipment, in the experiment two dynamometers, multi-channel amplifier and measuring computer were used (Fig. 4).

Table 1 - Chemical Composition of High-alloy Steel Č.4574

C	Si	Mn	Cr	N_i	M_0	T_i	P	S
(%)								
0.07	0.95	1.75	18.00	11.50	2.00	0.425	0.035	0.020

Table 2 - Material Properties of High-alloy Steel Č.4574

$R_{0.2}$	R_m	HB	A_m	A	Z	$\bar{r}$
(N/mm^2)		(daN/mm^2)	-	(%)		-
221.1	594.4	252.5	0.395	46.03	55.35	0.92
$\bar{\sigma} = 1196.1\bar{\varphi}^{0.333}$; $\bar{\sigma} = 221.1 + 1001.9\bar{\varphi}^{0.454}$						

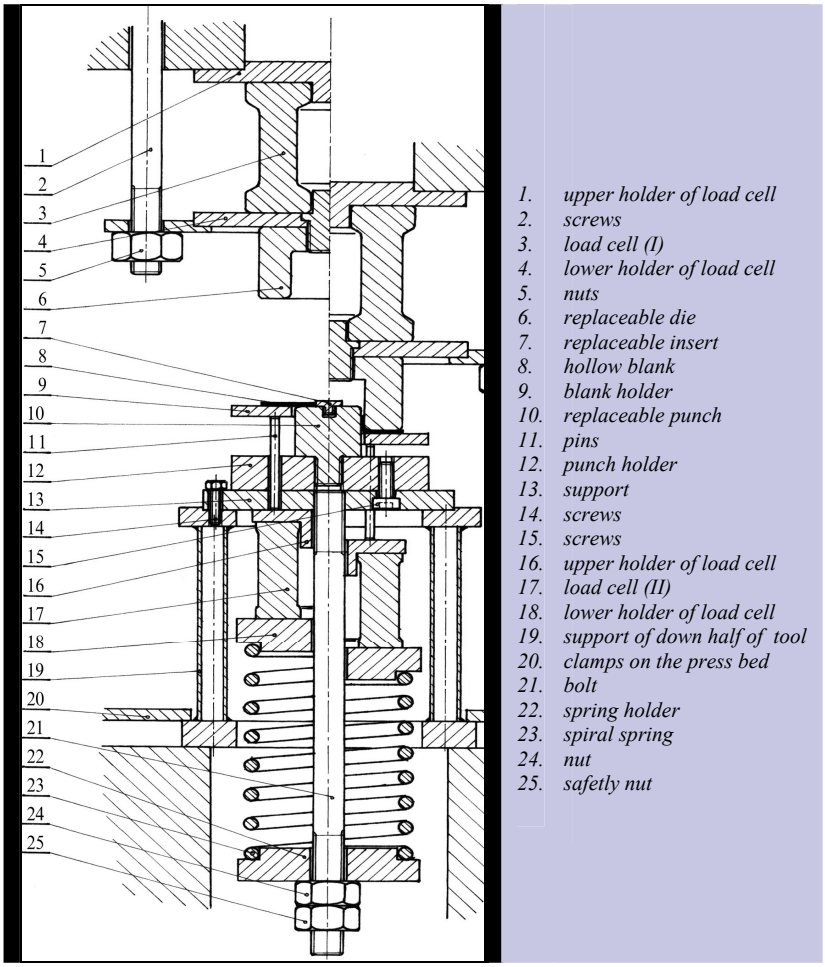

Fig. 3 - Experimental Set-up for Hole-flanging Process

Fig. 4 - Hydraulic Press with Measuring Equipment

3.2. Experimental Determination of the Hole-flanging Working Stress

To meet the needs of this research, forty separate series of experiments were carried out. For the each individual test, the diagram of punch force-punch stroke was recorded (Fig. 5).
Diagrams of the punch force-punch stroke have a characteristic shape with a prominent maximum as confirmed by the research done by other authors [3], [4]. Firstly, the punch force increased with punch displacement. After the maximum punch force had been obtained, the force decreased progressively with expansion of the hole and thinning of the blank. It is also obvious that the maximum punch force increases remarkably with the flanging ratio.
These diagrams point to the fact that the hole-flanging process belongs to typical non-stationary forming processes. The initial data and experimental results are given in Table 3. On the basis of experimental data and relation (11) the experimental values of the hole-flanging working stress are defined.

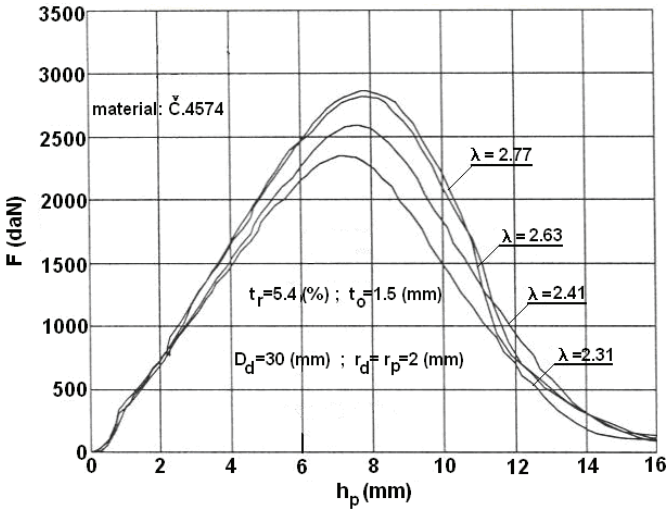

Fig. 5 - Force-Stroke Diagrams at various Flanging Ratios

Table 3 - The Initial Data and Experimental Results

material: Č.4574 ; flow curve: $\overline{\sigma} = 221.1 + 1001.9\,\overline{\varphi}^{0.454}$; friction coefficient: $\mu \approx 0.22$									
No	**t_0 (mm)**	**D_d (mm)**	**r_d (mm)**	**D_p (mm)**	**r_p (mm)**	**d_0 (mm)**	**t_r (%)**	**λ (-)**	**σ_{max} (N/mm^2)**
1	1.5	30	2	27	2	12	12.5	2.31	174,8
2	1	30	2	28	5	12	8.33	2.37	153,3
3	1	30	2	28	2	12	8.33	2.37	187,8
4	1.5	30	2	27	2	11.5	13.04	2.41	192,9
5	1	40	2	38	5	18.5	5.41	2.08	148,1
6	1	40	2	38	2	18.5	5.41	2.08	176,9
7	1	40	2	38	2	18	5.55	2.14	188,8
8	1	40	2	38	5	18	5.55	2.14	178,8
9	1	40	2	38	2	17.5	5.71	2.20	195,4
10	1	40	2	38	5	17.5	5.71	2.20	184,6
11	1.5	40	2	37	2	17	8.82	2.22	188,5
12	1	40	2	38	2	17	5.88	2.26	191,0
13	1.5	40	2	37	5	16.5	9.09	2.29	171,3
14	1.5	40	2	37	2	15.5	9.67	2.43	190,3
15	1.5	40	2	37	5	15	10	2.51	182,9
16	2	30	2	26	5	11	18.18	2.45	167,2
17	2	30	2	26	2	11	18.18	2.46	202,6
18	1	30	2	28	2	11.5	8.7	2.47	198,8
19	1.5	30	2	27	2	10.5	14.29	2.63	210,2
20	1	30	2	28	5	10.5	9.52	2.70	180,6
21	2	30	2	26	5	10	20	2.70	184,4
22	2	30	2	26	2	10	20	2.70	217,0
23	1	30	2	28	2	10.5	9.52	2.71	214,8
24	1.5	30	2	27	2	10	15	2.77	213,3
25	1	30	2	28	5	10	10	2.84	180,0
26	2	30	2	26	5	9.5	21.05	2.84	190,6
27	2	30	2	26	2	9.5	21.05	2.84	225,6
28	1	30	2	28	2	10	10	2.85	218,0
29	1.5	40	2	37	2	15	10	2.52	204,7
30	2	40	2	36	5	14.5	13.79	2.56	205,8
31	2	40	2	36	5	14	14.29	2.64	214,6
32	2	40	2	36	2	14	14.29	2.65	242,3
33	2	40	2	36	5	13.5	14.81	2.74	226,7
34	2	40	2	36	2	13.5	14.81	2.74	243,1
35	2.5	40	2	35	2	13.5	18.52	2.69	242,8
36	2.5	40	2	35	2	13	19.23	2.79	246,6
37	2.5	40	2	35	5	12.5	20	2.90	215,1
38	2.5	40	2	35	2	12.5	20	2.90	247,6
39	2.5	40	2	35	5	12	20.83	3.02	217,0
40	2.5	40	2	35	2	12	20.83	3.02	254,8

Comparative results of calculation and experiment are given in Fig. 6. The good agreement of the experimental and theoretical results validates the correctness of the mathematical model.

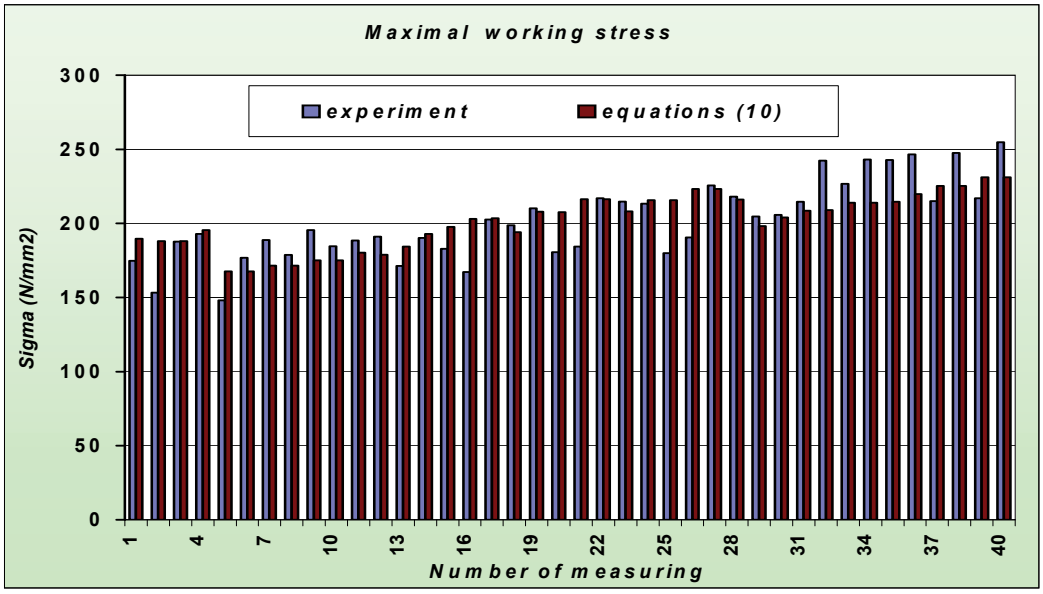

Fig. 6 - Comparative Results of Calculation and Experiment

3.3. Experimental Determination of the Limiting Flanging Ratio

As a criterion for determining the LFR the emergence of the first initial crack at the edge of the flanged neck is chosen. The outlook of the blanks used in the experiment and a series of finished parts are given in Fig. 7. The experimental research of the author of this paper and of other scientists point to two facts. Firstly, that t_r is the most influential factor, and, secondly, that (regardless of the kind of the used material) λ_{lim} is a monotonously rising function of the reduced sheet metal thickness.

In the concrete case, taking into account the influence of only the above-mentioned factor, the following regression equation was obtained after processing the experimental data:

$$\lambda_{lim} = (151.542 + 157.15\, t_r - 9.17\, t_r^2 + 0.23\, t_r^3)\, 10^{-3} \tag{16a}$$

Respecting the influence of the other geometric factors and their interactions, for the same experimental data, the adequate regression equation is obtained:

$$\lambda_{lim} = 1.9655 + 0.0397 t_r - 0.0519 r_{dr} - 0.0627 r_{pr} + 0.0078 t_r\, r_{dr} + 0.0010 t_r\, r_{pr} + 0.0357 r_{dr}\, r_{pr} \tag{16b}$$

A comparative analysis of the above-mentioned regression equations brings about the conclusion that equation (16b) is somewhat more accurate, but inadequate for engineering calculations due to heir complexsity. As can be seen from Fig. 8, equation (16a) provides for sufficient accuracy for practical calculations.

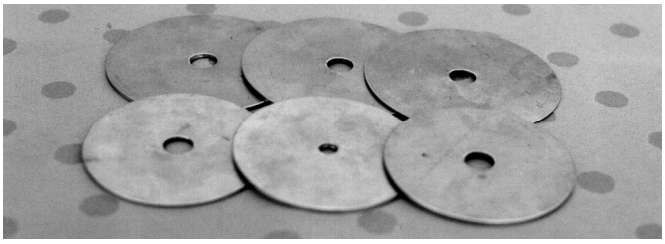

a)

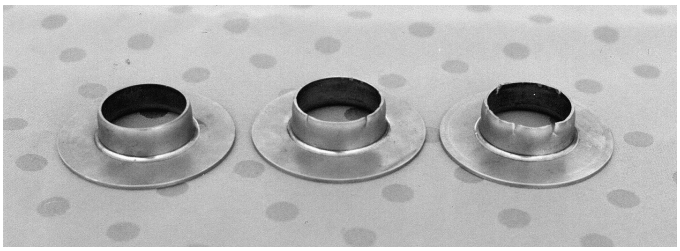

(I) (II) (III)

b)

Fig. 7 - Outlook of the Specimens before (a) and after Hole-Flanging (b):
$t_0 = 2mm\,; D_p = 36mm\,; r_d = 2mm\,; r_p = 5mm$
$(I)\,\lambda = 2.55\,; (II)\,\lambda_{lim} = 2.64\,; (III)\,\lambda = 2.74$

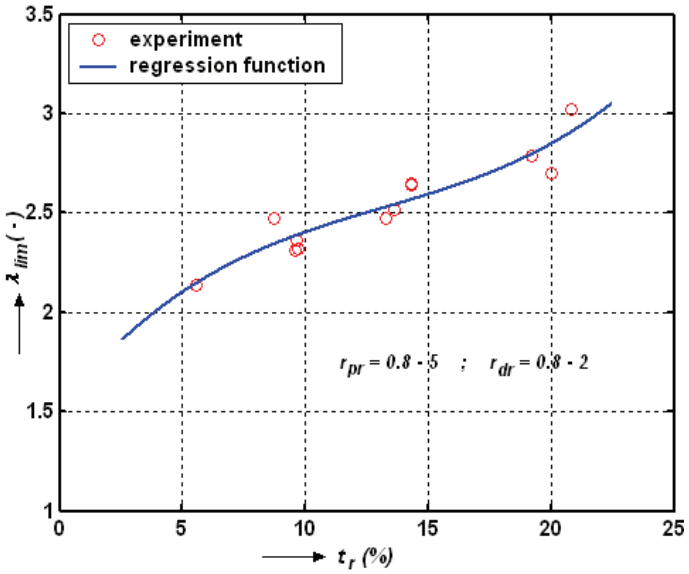

Fig. 8 - Dependence of the Limiting Flanging Ratio on the Reduced Sheet Metal Thickness

High limiting flanging ratios ($\lambda_{lim} = 2 \div 3$) confirm that the chosen material possesses high formability (flangeability). Such limiting flanging ratios provide for the production of flanged hollows of greater heights.
When it is not possible to obtain the desired the height of the flanged neck, the forming is done in two operations. In the first one, the deep drawing of the blank with a smaller hole is done, while in the other the pure hole-flanging is to be performed (enlarging of the hole at the bottom of the drawn cup). On the other hand, according to the definition of LFR, the re-penetration operation could be better than the direct hole-flanging process [19].

4. CONCLUSION

In this study conventional hole-flanging process is investigated theoretically and experimentally. The original formulae (10) for calculating working stress of the hole-flanging are derived. The theoretical results are compared to the experimental ones thereby their satisfying compliance is identified. For deviations of the theoretical from the experimental results the following reasons can be stated: (a) incompliance of the factual with the assumed stress/strain state (in some cases), (b) errors while determining the flow curve, (c) errors in estimating friction coefficient, (d) calculation with averaged values of the sheet metal thickness and flow stress, (e) errors in measurements, etc.
The LFR is the most important parameter of this forming process. On the basis of the analysis carried out in this paper it can be concluded that semi-empirical relations (16) are sufficiently accurate for practical calculations. When it comes to experimental research for concrete material, the regression equation in the form of cubic function (16a) can be recommended. The LFR is most affected by the reduced sheet metal thickness. Slight dissipation of the experimental points with respect to the regression curve reveals small impact of the other factors.
The results presented in this paper can be useful for engineers in designing hole-flanging process.

Nomenclature

$R^{'},\rho,\theta,\varphi$ - toroidal coordinates, $\sigma_\rho,\sigma_\theta,\sigma_\varphi...$ - components of stress tensor, $\varepsilon_\rho,\varepsilon_\theta,\varepsilon_\varphi....$ - components of strain tensor, $u_\rho,u_\theta,u_\varphi$ - components of total velocity, $\overline{\sigma},\overline{\sigma}_{ave}$ - flow stress, average flow stress (efective stress), respectively, $\overline{\sigma}_0 \cong R_{0.2}$ - initial flow stress (yield strenght), R_m - ultimate tensile strength, A_m – uniform elongation, C - characteristic stress (material constant), n - strain hardening coefficient, $\overline{\varphi}$ - logarithmic (natural) strain, ψ_m - uniform deformation of the cross-section in the simple tensile test, F_{max} - maximal force of hole-flanging, σ_{max} - maximal working stress of hole-flanging, D_0 - initial outer blank diameter, d_0 - initial inner blank diameter, t_0 - initial blank thickness, t,h,D - wall thickness, height and average diameter of the finished part, H,H_1,D_1 - geometrical parameters (see Fig.1), $\bar{t}$ - average thickness of flanged neck $(\bar{t} \approx 0.5(t_0 + t_1))$, t_1 - wall thickness at the edge of flanged neck, d_i - current inner workpeace diameter, d_{im} - inner workpeace diameter at the moment of full envelopment of the punch edge $(\varphi = \pi / 2)$, D_p,r_p - punch diameter and punch-corner radius, respectively, D_d, r_d - die diameter and die-corner radius, respectively, r_f - radius of flanged neck ($r_f \cong r_d$), α - current workpeace

semi-angle $(\alpha = \pi/2 - \varphi)$, (see Fig. 2), λ, λ_{lim} - flanging ratio $(\lambda = D/d_0)$ and limiting flanging ratio $(\lambda_{lim} = D/d_{0\,min})$, respectively, t_r - reduced initial blank thickness $(t_r = 100 \cdot t_0/d_0)$, r_{dr} - reduced die-corner radius $(r_{dr} = r_d/t_0)$, r_{pr} - reduced punch-corner radius $(r_{pr} = r_p/t_0)$, P - 'P-criterion', μ - friction coefficient, $\bar{r}$ - average anisotropy coefficient, h_p - punch stroke.

REFERENCES

[1] Johnson W., Ghosh S. K., Reid S. R.: Piersing and hole-flanging of sheet metals: a survey. Memoires scientifiques revue metallurgie, 4, 1980, pp. 585-606.

[2] Schmoeckel D., Schlagau S.: Verbesserung der Verfahrensgrenzen beim Kragenziehen durch Überlagerung von Druckspannungen. Annals of the CIRP, Vol. 37/1, 1988, pp. 271-274. (in English).

[3] Huang Y.M., Chien K.H.: Influence of the punch profile on the limitation of formability in the hole-flanging process. Journal of Materials Processing Technology, 113, 2001, pp. 720-724.

[4] Huang Y.M., Chien K.H.:. The formability limitation of the hole-flanging process. Journal of Materials Processing Technology, 117, 2001, pp. 43-51.

[5] Marinković V., Nikolić J., Rančić B.: Analysis of hole-flanging process in stainless steel sheet. Journal for Tehnology of Plastcity, Vol. 26, No 1, 2001, pp. 57-66.

[6] Hyun D.I., Oak S.M., Kang S.S., Moon Y.H.: Estimation of hole flangeability for high strength plates. Journal of Materials Processing Technology, 130/131, 2002, pp. 9-13.

[7] Hu P., Li D.Y., Li Y.X.:. Analytical models of strech and shrink flanging. International Journal of Machine Tools & Manufacture, 43, 2003, pp. 1367-1373.

[8] Marinković V., Nikolić J.: Experimental-analytical method of determing working stress of the hole-flanging upon steel sheet parts. 3nd Iternational Conference RaDMI 2003, Herceg Novi, 2003, pp. 332-337.

[9] Chen T.C.: An analysis of forming limit in the elliptic hole-flanging process of sheet metal. Journal of Materials Processing Technology, 192/193, 2007, pp. 373-380.

[10] Li D., Luo Y., Peng Y., Hu P.: The numerical and analytical study on stretch flanging of V-shaped sheet metal. Journal of Materials Processing Technology, 189, 2007, pp. 262-267.

[11] Kumagai T., Saiki H., Meng Y.: Hole flanging with ironing of two-ply thick sheet metals. Journal of Materials Processing Technology, 89/90, 1999, pp. 51-57.

[12] Lin H.S., Lee C.Y., Wu C.H.: Hole flanging with cold extrusion on sheet metals by FE simulation. International. Journal of Machine Tools & Manufacture, 47, 2007, pp. 168-174.

[13] Thipprakmas S., Jin M., Murakawa M.: Study on flanged shapes in fine blanked-hole flanging process (FB-hole flanging process) using finite element method (FEM). Journal of Materials Processing Technology, 192/193, 2007, pp. 128-133.

[14] Marinković V.: Analysis of the process of the reversibile and combined deep drawing. Journal for Technology of Plasticity, Vol. 18, No 1-2, 1993, pp. 39-50.

[15] Storozhev M. V., Popov E. A.: Teoriya obrabotki metallov davleniem. ''Mashinostroenie", Moscow, 1977, 423 pp. (in Russian).

[16] Panknin W.: Die Grundlagen des Tiefziehens im Anschlag unter besonderer Berücksichtigung der Tiefziehprüfung. Bänder-Bleche-Rohre, 4, 5, 6, 1961, s. 133-143, 201-211, 264-271 (in German).

[17] Popov E. A.: Osnovy teorii listovoy shtampovki. "Mashinostroenie", Moscow, 1977, 278 pp. (in Russian).

[18] Averkijev A. J.: Ocenka shtampuemosti listovogo prokata. "Kuznechno - shtampovochnoe proizvodstvo", No 10, 1987, pp. 6-8. (in Russian).

[19] Li C.L., Huang Y.M., Tsai Y.W.: The analysis of forming limit in re-penetration process of the hole-flanging of sheet metal. Journal of Materials Processing Technology, 201, 2008, pp. 256-260.

ODREĐIVANJE RADNOG NAPONA I GRANIČNOG ODNOSA PROVLAČENJA U PROCESU ŠUPLJEG PROVLAČENJA LIMENIH ELEMENATA

Velibor Marinković
Univerzitet u Nišu, Mašinski fakultet, Niš, Srbija

REZIME

Šuplje provlačenje spada u najvažnije procese deformisanja, široko primenjivan u proizvodnji limenih elemenata u automobilskoj i elektro industriji.
Šuplje provlačenje se primenjije uglavnom iz dva razloga: (a) radi podizanja krutosti limenih delova (struktura) i/ili (b) radi formiranja grla na limenim elementima ili cevima u cilju njihovog povezivanja sa drugim elementima (direktno ili pomoću narezanog navoja).
Šuplje provlačenje se realizuje tako što se slobodan deo limenog pripremka, sa malim otvorom u sredini, pod dejstvom provlakača uvlači u otvor matrice radi formiranja grla, čiji je prečnik znatno veći od prečnika inicijalnog otvora. U početnoj fazi ovaj proces je sličan dubokom izvlačenju.
Dijagram sile, sa izraženim maksimumom, ukazuje da šuplje provlačenje spada u tipične nestacionarne procese deformisanja. Odlikuje ga složeno naponsko-deformaciono stanje. U radu je izveden originalni obrazac za proračun radnog napona, na osnovu kojeg se određuje maksimalna sile šupljeg provlačenja. Valjanost matematičkog modela i izvedenih jednačina verifikovani su eksperimentalno.
Odnos provlačenja je najvažniji geometrijski parametar procesa šupljeg provlačenja, jer utiče progresivno na silu i utrošeni deformacioni rad. S druge strane, sa povećanjem odnosa provlačenja povećava se i visina istisnutog grla, što je veoma značajno kada se radi o spajanju datog limenog elementa sa drugim delovima.
Granični odnos provlačenja je mera sposobnosti konkretnog materijala da se deformiše šupljim provlačenjem. U radu su date empirijske jednačine za proračun graničnog odnosa provlačenja, koje su u zadovoljavajućoj saglasnosti sa eksperimentalnim podacima.